How climate change may shift power demand in Japan: insights from data-driven analysis

Léna Gurriaran[1, 2], Katsumasa Tanaka[1,3], Kiyoshi Takahashi[4], Philippe Ciais[1]

[1] Laboratoire des Sciences du Climat et de l'Environnement (LSCE), IPSL, CEA/CNRS/UVSQ, Université Paris-Saclay, Gif-sur-Yvette, France

[2] Atos, River Ouest, 95877 Bezons cedex, France

[3] Earth System Division, National Institute for Environmental Studies (NIES), Tsukuba, Japan

[4] Social Systems Division, National Institute for Environmental Studies (NIES), Tsukuba, Japan

Abstract

The impact of climate change on power demand in Japan is a matter of concern for the Japanese authorities and power companies as it may have consequences on the power grid. We trained random forest models against daily power data in ten Japanese regions and for different types of power generation to project changes in future power production and its carbon intensity. To do so, we used twelve predictors: six climate variables, five variables accounting for human exposure to climate, and one variable for the level of human activities. We then used the models trained from the present-day period to estimate the future power demand, carbon intensity, and pertaining CO_2 emissions over the period 2020-2100 under three SSPs scenarios (Shared Socioeconomic Pathways: SSP126, SSP370, and SSP585). The impact of climate change on CO_2 emissions via power generation shows seasonal and regional disparities. In cold regions, a decrease in power demand during winter under future warming leads to an overall decrease in power demand over the year. In contrast, the decrease in winter power demand in hot regions can be overcompensated by an increase in summer power demand because of more frequent hot days, leading to an overall annual increase. From our regional models, the power demand

should increase the most in most Japanese regions in May, June, September, and October and not in the middle of summer, as has been found in older studies. Such an increase could result in regular power outages during those months if not considered, as the power grid could be particularly tense. Overall, we observed that power demand in regions with extreme climates is more sensitive to global warming than in temperate regions. The impact of climate change on power demand induces a net annual decrease in CO_2 emissions in all regions except for Okinawa, in which power demand strongly increases during the summer, resulting in a net annual increase in CO_2 emissions. However, climate change's impact on carbon intensity may reverse the trend in some regions (Shikoku, Tohoku). We also assessed the relative impacts of socioeconomic factors such as population, GDP, and environmental policies on CO_2 emissions. When combined with these factors, we found that the climate change effect is more important than when considered individually and significantly impacts total CO_2 emissions under SSP585.

Context and Scale

After the adoption of the Paris Agreements in 2015, aiming at limiting warming under 2°C by reducing greenhouse gas emissions, decarbonizing the energy mix became a major issue. As the third largest economy in the world, Japan has made ambitious commitments: -26% of greenhouse gas emissions between 2030 and 2013 and reach net zero by 2050. However, 80% of Japan’s power generation still comes from fossil fuels. This study explores the impact of climate change on Japan’s power grid and CO_2 emissions from power generation through data-driven models that project power demand and carbon intensity with climate change. We also account for the impact of population, GDP, and environmental policies aiming to decarbonize the energy mix. Japan provides a good case study, offering insights into what could happen at the global scale, as it has ten regions covering a wide range of climates.

1. Introduction

Many studies have investigated the impact of climate change on energy systems. According to the review of Yalew et al. (2020), a slight decrease in hydropower and thermal energy capacity at a global scale is expected. However, the impact of climate on power demand strongly varies across regions (Auffhammer, M., Baylis, P., & Hausman, C.H. (2016); Van Ruijven, De Cian, and Wing, 2019; Gurriaran et al., 2022). Van Ruijven, De Cian, and Wing (2019) found that the energy demand could increase by 25% in the tropics by 2050 due to increasing hot days, whereas higher latitudes are more prone to a decline in energy demand.

This study focuses on power demand, which comprises a significant percentage of the total energy demand. Power demand is closely related to meteorological conditions, and there is an increasing concern over how it will respond to changing climate. According to Yalew et al. (2020), a global increase in cooling demand and a decrease in heating demand are expected. For example, heat waves are becoming more frequent and intense in hot regions (Zittis et al., 2021), causing increased peak demand during those events. The potential power outages that may result from increased peak demand are a matter of concern for health systems (Patel et al., 2022). Depending on the scenario of socioeconomic development, 2 to 5 billion people are at risk of facing deadly heat and are unable to afford air conditioning systems (Mora et al., 2017; Andrijevic et al., 2021). CO_2 emissions from power generation constitute a further consequence of climate-induced changes in power demand. An increase in demand for air conditioning and, thus, power generation in subtropical latitudes will subsequently increase the amount of CO_2 emissions from these regions. However, this effect may be counterbalanced at a global scale by a decrease in heating demand in high latitudes leading to lower CO_2 emissions. Our study addresses this phenomenon specifically in Japan.

Japan is one of the largest economies in the world, with the third-largest Gross Domestic Product (GDP) internationally (IMF, 2022). In 2020, power generation reached 987 TWh, *i.e.,* 7.9 MWh per capita (IEA, 2020), ranking the country in the top 20 largest consumers of electricity per capita in the world. The residential sector is the third largest sector for power demand in Japan, after commercial and public services and industry. Japan comprises a territory ranging from 46° to 20° north (2200 km long from northeast to southwest), and *de facto* includes a wide range of climates, from humid continental to subtropical. The country is divided into ten distinct geographical areas administered by designated power companies. Each region is characterized by a specific climate, population density, urbanization rate, GDP per capita, *etc.,* all factors determining power demand. For example, the adoption rate of household air conditioning is around 90% on a national scale (De Cian et al., 2019), but it varies across regions from north to south. Whereas fewer homes are equipped with cooling systems in Hokkaido, where heating needs are more important, the tropical climate in Okinawa induces a strong demand for air conditioning. Although 80% of the nation's power is produced with fossil fuels (IEA, 2022), some regions use more renewables than others. Each region thus has a specific carbon intensity for power generation depending on the energy mix used by the local power company.

We use Japan as a case study to investigate how climate change can influence CO_2 emissions by changing power demand and influencing the carbon intensity of the energy mix. We analyze climate change impacts at national and regional scales and develop regional statistical models to derive monthly and seasonal trends and annual net changes in CO_2 emissions until 2100. These models incorporate the effects of climate change and specific regional socioeconomic factors (population, GDP, and environmental policies aiming to decarbonize the energy mix) to project power demand, carbon intensity, and CO_2 emissions. Detailed energy mix and climate data are available homogeneously for all ten regions. Hiruta et al. (2022a) used similar data to develop a method that acquires regional temperature response functions (TRFs) for power demand and investigates the effect of climate change on power demand. Although our method to obtain regional models projecting power demand is similar to Hiruta et al. (2022a), we use more up-to-date climate

data for the projections: our climate variables are from the last phase of the CMIP project, CMIP6, instead of CMIP5 for the Hiruta study. Unlike the Hiruta study, we further explore long-term changes in CO_2 emissions that can be caused by changes in power demand and carbon intensity under future climate and socioeconomic scenarios.

Section 2 details the data used and the algorithms tested to develop models that simulate power demand and carbon intensity. It also describes the method to calculate CO_2 emissions under three future scenarios: SSP1-2.6, SSP3-7.0, and SSP5-8.5. Section 3 presents the results; it describes the regional relationships between predictive variables and power demand and carbon intensity, details the regional and temporal impact of climate on power demand, carbon intensity, and CO_2 emissions, compares our results to those of Hiruta et al. (2022b) and discusses the relative importance of climate and socioeconomic factors in determining the power demand, carbon intensity, and CO_2 emissions. Section 4 discusses the results under a broader context, including caveats of our study. Section 5 concludes the paper.

2. Data and methods

The work presented in this article is built around three main steps (Figure 1): i) model development and selection, ii) projections of power demand and carbon intensity under future climate scenarios, and iii) projections of CO_2 emissions under future climate and socioeconomic scenarios. This section details the datasets needed for the different steps (Table 1), the model development, and the projection stage.

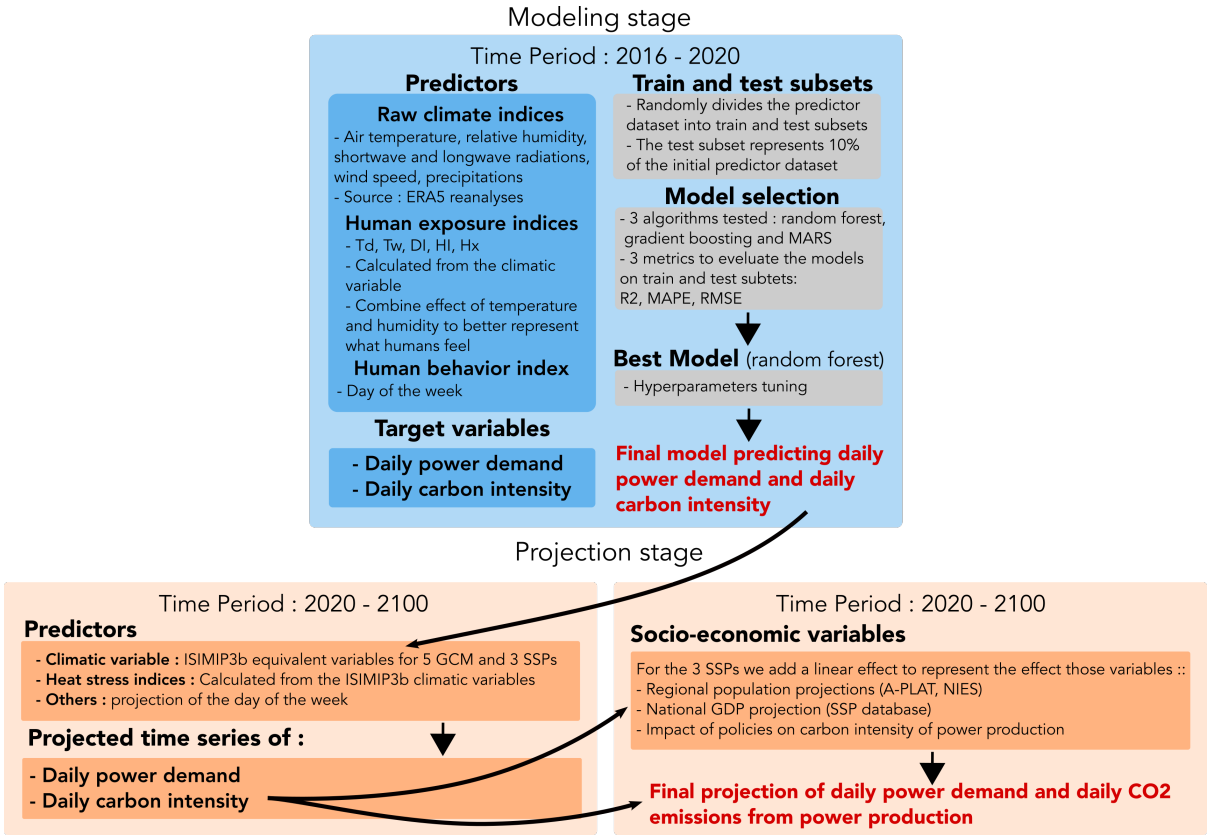

Figure 1. Flowchart of the methodological procedures used in this study.

Variable and description	ERA5		ISIMIP3b	
	name	*unit*	*name*	*unit*
Near surface atmospheric temperature (2m above the surface)	T2M	K	TAS	K
Relative Humidity (water vapor pressure as a percentage of the value at which the air becomes saturated)	RH	$\%$	HURS	$\%$
Surface solar radiation downward (amount of shortwave radiation that reaches a horizontal plane at the surface)	SSRD	$J.m^{-2}$	RSDS	$W.m^{-2}$
Surface thermal radiation downward (amount of longwave radiation emitted by the atmosphere and clouds that reaches a horizontal plane at the surface)	STRD	$J.m^{-2}$	RLDS	$W.m^{-2}$
Wind (speed of horizontal wind 10 m above the surface)	U = $\sqrt{u_{10}^2 + v_{10}^2}$	$m.s^{-1}$	SFCWIND	$m.s^{-1}$

Variable and description	ERA5		ISIMIP3b	
	name	*unit*	*name*	*unit*
Near surface atmospheric temperature (2m above the surface)	T2M	K	TAS	K
Relative Humidity (water vapor pressure as a percentage of the value at which the air becomes saturated)	RH	$\%$	HURS	$\%$
Precipitation (total amount of water that fall at the surface)	TP	m	PR	$kg.m^{-2}.s^{-1}$

Table 1. Current (ERA5 for training) and future (ISIMIP3b for projections) climate data used in our analysis.

2.1 Training data

We trained a statistical model on climate reanalysis data from the ERA5 project (Muñoz Sabater, 2019) to reproduce the observed daily power demand and carbon intensity for all ten regions. Six raw climate variables were used as predictors: temperature, relative humidity, solar and thermal radiation, wind, and precipitation (Table 1). Those data were downloaded from the Climate Data Store website (CDS 2022) at an hourly time resolution over the period 2016 - 2020 and a spatial resolution of 0.08° and then aggregated as daily and regionally averaged values. Five human exposure indices were calculated from these climate variables and also used as predictors: the dew point temperature at which the air is saturated with water vapor (T_d), the wet bulb temperature (T_W), which is the lowest temperature to which air can be cooled by water evaporation, the discomfort index, which is often used to calibrate air conditioner (DI), the Humidex (Hx), which explains what the temperature feels like for the human body and the Heat Index (HI), which represents what the combination of temperature and relative humidity feels like for the human body. Equations used to calculate these indices (Thom, 1959; Sohar et al., 1963; Stathopoulou et al., 2005; Epstein et al., 2006; Buzan et al., 2014; Maia-Silva et al., 2020) are detailed in supplementary materials (Section S1). We also used the days of the week (DOW) as a proxy for human activity. Each day is assigned a numerical value to quantify its effect in our models: Monday is 0, Tuesday 1,..., and Sunday 6.

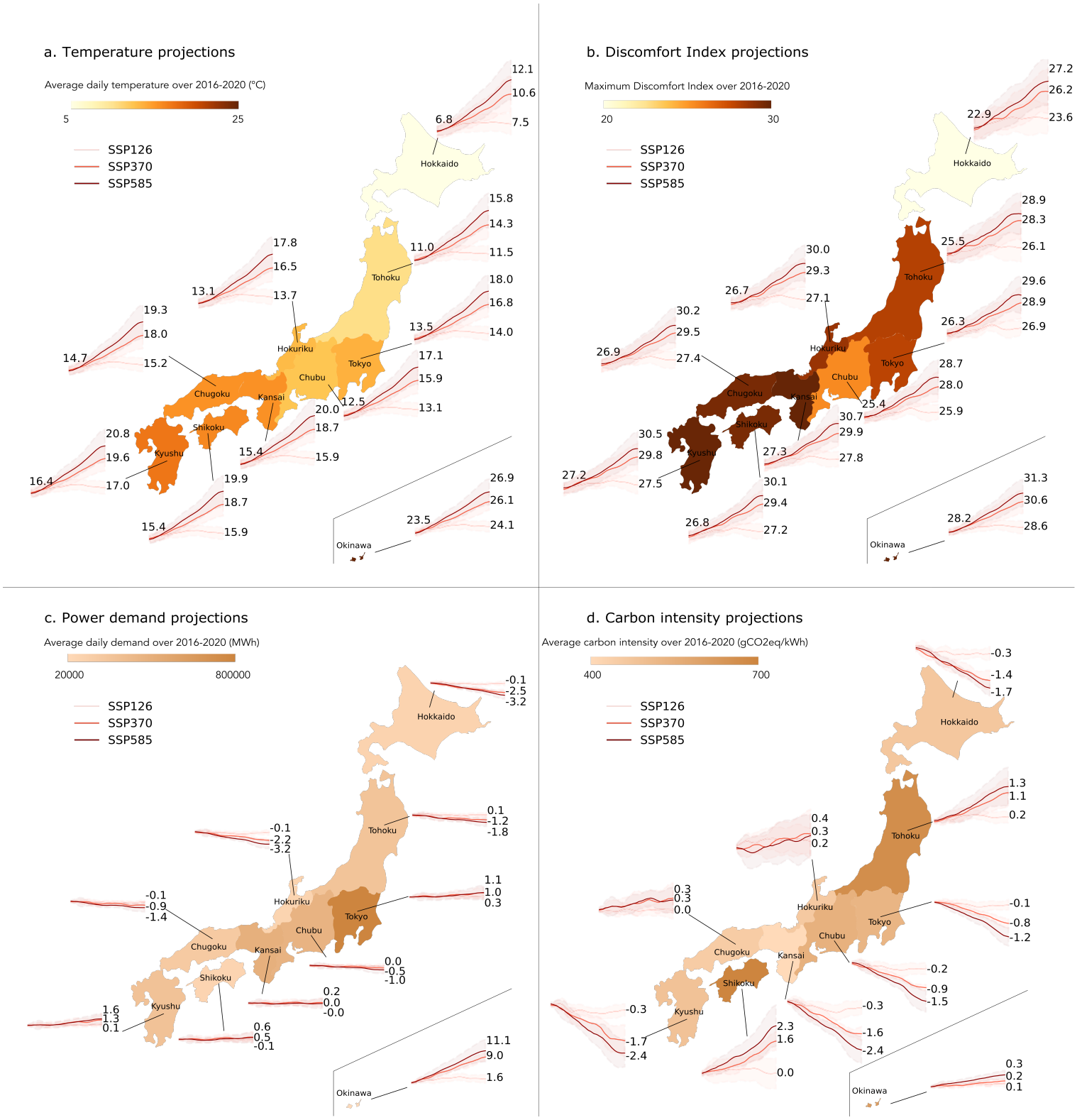

Figure 2. Current and future projections under climate change of average daily temperature (a), DI (b), power demand (c), and carbon intensity (d) for the ten regions of Japan. The color scale on the maps indicates the level for the period 2016-2020. Projections for the period 2020-2100 are shown in solid bands. Lines give mean values from five models; shaded areas show standard deviations. Future projections in panels c and d are shown in percentage (relative changes to present levels).

Hourly data for power demand and the energy mix was obtained directly from the website of the ten power utilities (supplementary materials, Section S2). Data have been available since April 2016 and provided for eight types of power supply: fossil, nuclear, photovoltaic, wind, hydroelectricity, geothermal, biomass, and pumped-storage hydroelectricity. The energy mix of each region is detailed in supplementary materials (Section S2). Further details on the types of fossil fuel (coal, gas, and oil share) are unavailable at the hourly scale. Still, the Japanese agency for natural resources and energy from the Ministry of Economy, Trade, and Industry (METI) provides monthly fractions of coal, gas, and oil used in the regional energy mixes from 2017 to 2020. The fossil energy mix is relatively constant over these four years, with approximately 50% of gas, 40% of coal, and 10% of oil. The regional daily carbon intensity of power generation was calculated assuming this ratio constant.

2.2 Model development and selection

We tested three non-parametric models of daily power demand and carbon intensity; random forest classifier (Ho, 1995; Breiman, 2001), histogram-based gradient boosting (Friedman, 1999), and Multivariate Adaptive Regression Spline (MARS) (Friedman, 1991). We trained the algorithms for all ten regions with twelve predictors: six climate variables, five human exposure indices, and human activity proxy (DOW), all twelve described in section 2.1. The training dataset represented 75% of the data, and the test dataset accounted for 25%. We evaluated the performances of the algorithms on both datasets using three metrics: the coefficient of determination (R2), the Mean Absolute Percentage Error (MAPE), and the Root Mean Square Error (RMSE).

Results are very similar between random forest and gradient boosting, and both algorithms perform better than the MARS algorithm (Table S2 and Figure S1, Section S3, supplementary materials). As random forests have fewer hyper-parameters to optimize, we decided to proceed with this algorithm for the projection stage. Although the methodology used for the model development and selection stage is the same as Hiruta et al. (2022a),

we developed our models with a different algorithm and used different evaluation metrics. We used partial dependence plots (PDPs) and Shapley values to interpret the regional models obtained with random forests and to show how each predictor affects the model outputs. PDPs were calculated from a subsample of fifty observations, and Shapley values were calculated for each observation of each predictor.

2.3 Projections

Once the regional models were calibrated for current climate conditions (*i.e.*, the period 2016-2020), we employed them to project the evolution of power demand and carbon intensity under different climate scenarios over 2020-2100 (Figures 2c and 2d). We worked with three scenarios (SSP1-2.6, SSP3-7.0, and SSP5-8.5) and used bias-corrected and statistically downscaled climate projections from the ISIMIP3b simulation round (Lange, 2021) at a daily timescale as predictors. Those data come from five different Earth System Models from the 6th phase of the CMIP project (CMIP6); GFDL-ESM4, IPSL-CM6A-LR, MPI-ESM1-2-HR, MRI-ESM2-0, and UKESM1-0-LL. Figure 2a shows the projected temperatures for all ten regions and three scenarios as an example of the projected climate predictors. We calculated human exposure indices (DI (Figure 2b), Hx, HI, Td, and Tw) from the projected climate predictors. Finally, we simulated daily climate-induced CO_2 emission projections by multiplying daily power demand and carbon intensity projections.

2.4 Socioeconomic scenarios

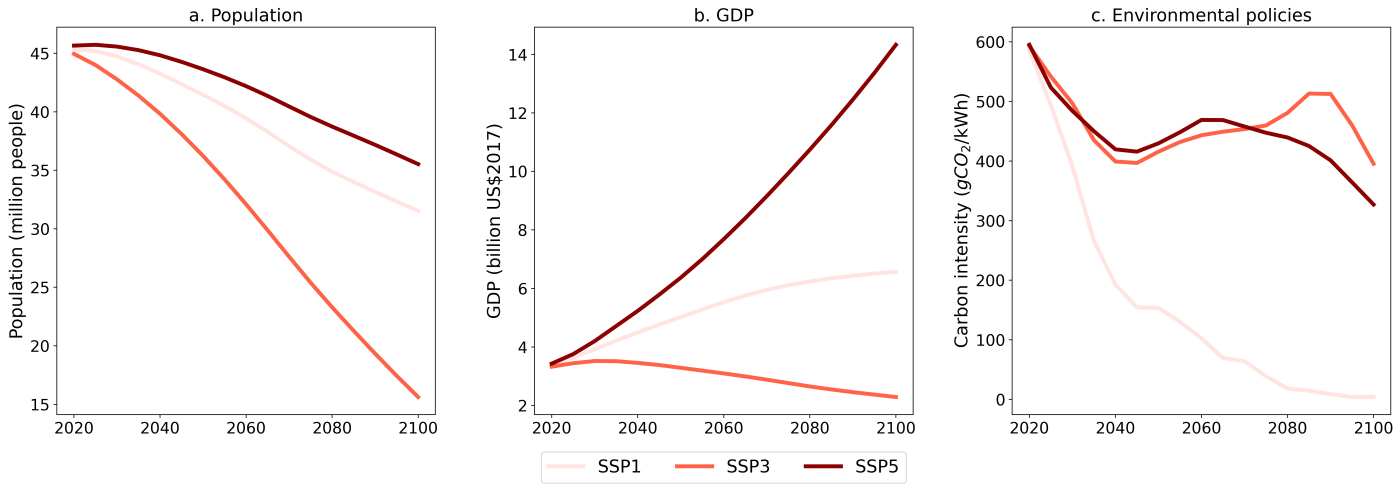

Figure 3. Socioeconomic projections of (a) population, (b) GDP, and (c) environmental policies aiming to decarbonize the energy mix used for power generation for the region of Tokyo.

The last step of our study was to include the impacts of socioeconomic factors on CO_2 emissions for all three SSPs. The Climate Change Adaptation Information Platform from the National Institute for Environmental Studies (NIES), Japan (A-PLAT, 2022), provides population projections at the prefecture scale. We aggregated such projections at the regional scale. Those data predict a decrease in Japan's population in all SSPs (Figure 3a). We obtained regional GDP projections (Figure 3b) by scaling Japan's GDP projections provided by the OECD (Riahi et al., 2017; Dellink et al., 2017) with current ratios between Japan's total GDP and regional GDP. Given the absence of regional GDP projections, we assumed that all regional GDP projections follow the same trend. We calculated Japan's carbon intensity projections (Figure 3c) based on national projections of the IMAGE3.2 model (Van Vuuren et al., 2021). We downscaled the national carbon intensity projection to regional levels with the same methodology as for GDP. Further details can be found in the supplementary material (Section S4). We quantified the individual influence of each factor (climate change, population, GDP, and environmental policies aiming to decarbonize the energy mix) on total CO_2 emissions by varying one factor at a time.

3. Results

3.1 Regional models: important features explaining daily power demand and carbon intensity variations in each region

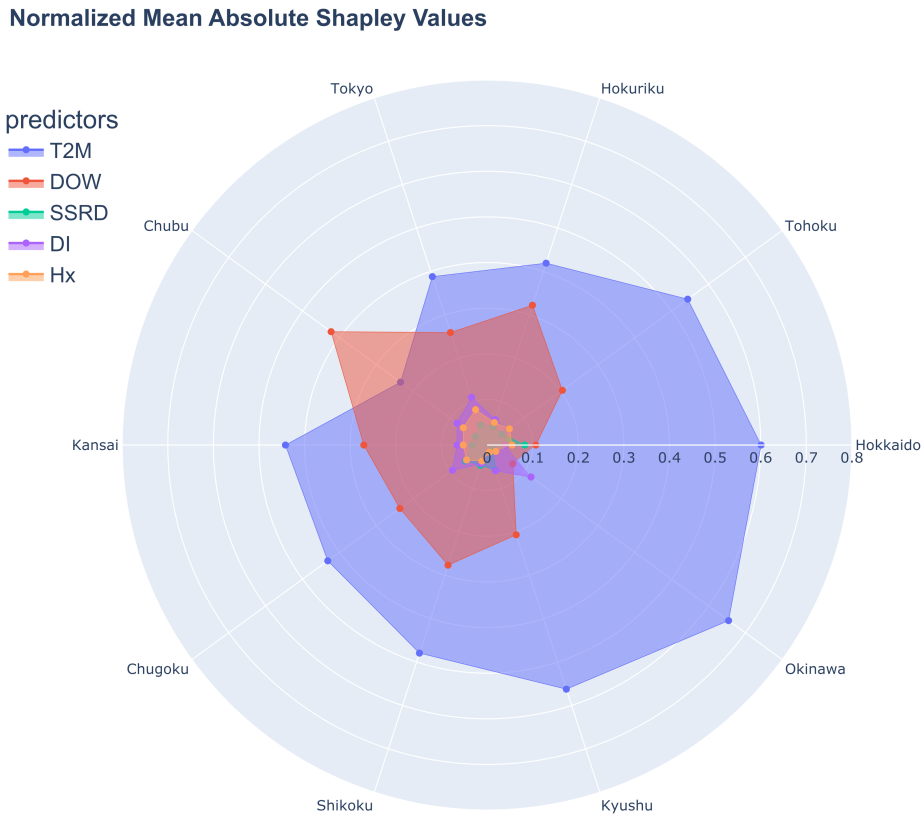

Figure 4. Radar plot showing the relative importance of the main predictors explaining power demand across regions (T2M, DOW, SSRD, DI, and Hx - see Table 1), obtained from the normalized mean absolute Shapley values of all observations for each predictor. The relative importance of the predictor is calculated for each region by normalizing the mean absolute Shapley value of every predictor.

We used global and local model-agnostic interpretability methods to analyze the effect of predictors on our model predictions. Such methods can be distinguished into global and local diagnostics. Global diagnostics allow understanding of the average behavior of a machine learning model, thus giving hints on the mechanisms that influence the prediction. PDPs are part of these diagnostics. Such plots show the marginal effect of one predictor on the model outputs (here, power demand or carbon intensity). PDPs are obtained by taking

the average of the Individual Conditional Expectation plots (ICE plots) lines. ICE plots represent one line per observation showing a change in the prediction when a predictor changes. Local diagnostics, such as Shapley values, explain individual predictions of a machine learning model. The interpretation of the Shapley values is that "*Given the current set of feature values, the contribution of a feature value to the difference between the actual prediction and the mean prediction is the estimated Shapley value"* (Molnar C., 2022). One can interpret Shapley values as a way to represent the probability of an impact of a predictor in the projection; a negative Shapley value shifts the predicted value in a negative direction, whereas a positive Shapley value shifts it in a positive direction.

We calculated Shapley values for all predictors in all ten regions. Of twelve predictors, five consistently appear among the most important to explain the power demand (Figure 4): the temperature (T2M), the day of the week (DOW), the solar radiation (SSRD), the discomfort index (DI) and the Humidex (Hx). T2M is the most important predictor in all regions except Chubu and Okinawa, followed by DOW. The order between T2M and DOW is reversed in Chubu. DI is the second most important predictor instead of DOW in Okinawa (Figure 4). The third most important predictor varies by region, but in general, it is DI (for six regions).

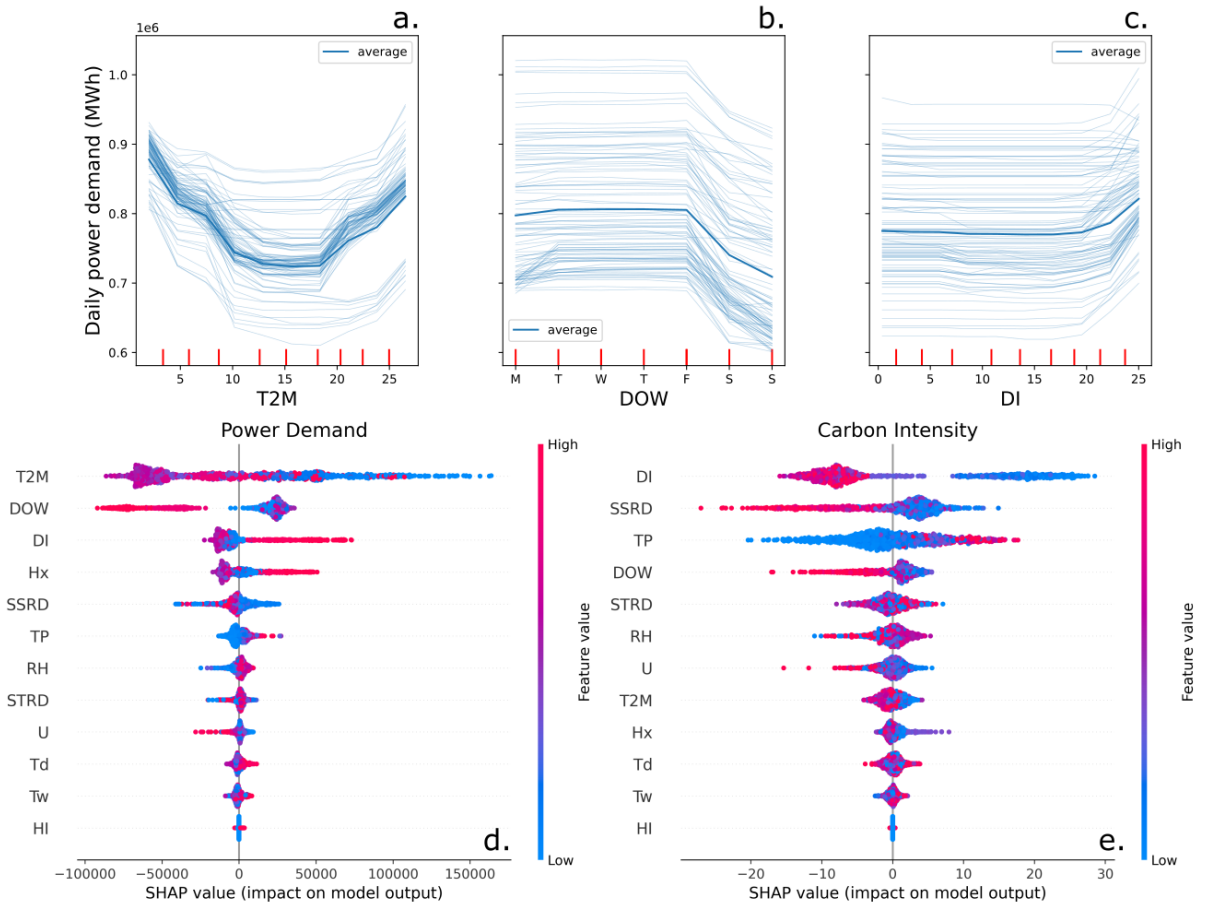

Figure 5. Partial dependence plot (thick line) and Individual Conditional Expectation plots (thin lines) for 100 model realizations for three main predictors explaining the power demand for the Tokyo region: air temperature at two meters above ground T2M (a), day of week DOW (b - the letters on the x-axis indicate the days of the week) and discomfort index DI (c). The vertical red bars show the predictor values distribution. The lower panels represent the Shapley values for each predictor for power demand (d) and carbon intensity (e). The figures for the other regions can be found in the supplementary material.

We looked at the PDPs of the main predictors and the Shapley values (Figure 5 and S2 in the supplementary materials) to better understand the non-linear influence of the predictors in our regional models. For example, with the Tokyo region, the PDP for T2M shows a U-shaped dependency of power demand to temperature (Figure 5a). Two temperature thresholds can be identified: power demand is increasing under 10 °C for heating purposes and above 18 °C for cooling purposes. The power demand is more or less constant between those two temperatures. Shapley values (Figure 5d) show that when temperature

values are either high or low (red and blue tones), power demand shifts in a positive direction, thus confirming the behavior observed with the partial dependence plot. The same relationship between temperature and power demand is also observed in several other regions (Figure S2, Section S5, supplementary materials). However, Hokkaido and Okinawa show different relationships. Power demand decreases when the temperature increases in Hokkaido and remains constant above 10°C, suggesting that power demand is controlled only by heating demand. The opposite effect is observed in Okinawa; power demand is constant under 24°C and increases once this temperature is exceeded. The specific regional thresholds triggering power demand for heating or cooling reflect households' structure and population behavior.

We also analyzed the dependency of power demand on the days of the week (DOW) with PDP and Shapley Values (Figures 5b and 5d). Power demand is constant from zero to four (Monday to Friday) and decreases above four, reflecting a lower demand during weekends. Figure 5d highlights the clear separation between weekends and working days. The same relationship is observed for all regions, although the impact of weekends on power demand is larger in Chubu (Figure S2e and Figure 4).

Finally, we analyzed the relationship between the DI and power demand (Figures 5c and 5d). Power demand increases when the threshold of 21 is exceeded. This behavior is observed for all regions having the DI as one of the three most influential predictors (Figure S2, supplementary material). Previous studies identified 21 as the threshold above which people start to feel heat stress (Thom, 1959; Stathopoulos et al., 2005), and DI is often used to calibrate air conditioners (Sohar et al., 1963; Epstein et al., 2006; Buzan et al., 2014; Maia-Silva et al., 2020), explaining such behavior.

We analyzed the relationships between carbon intensity and all 12 predictors with Shapley values (Figure 5e). In the example of Tokyo, DI is the most important predictor. It positively shifts carbon intensity predictions when the predictor values are low, meaning that more

fossil fuels are used for power generation when DI is low. Surface solar radiation downward (SSRD) is the second most important predictor. SSRD negatively shifts carbon intensity predictions when the SSRD value is high, probably because solar panels more easily exploit solar energy under a clear sky with much incoming solar radiation than under a cloudy condition. It should be noted that too strong solar radiation can inhibit the efficiency of power production from solar panels. Precipitation (TP) has the opposite effect. Carbon intensity predictions are shifted positively when TP is important, meaning less use is made of renewable energies. The order of importance of predictors for carbon intensity predictions varies more across regions than for power demand. However, more climate predictors are among the most important predictors, reflecting the dependency of the daily variability of the renewable energy capacity on the daily weather.

3.2 Impact of future climate change on power demand, carbon intensity, and CO_2 emissions

Power demand projections for all ten regions and three scenarios (Figure 2c, Section 2) show that climate change's impact on power demand differs between regions throughout the century. Such projections show a warming-induced decrease in power demand under SSP3-7.0 and SSP5-8.5 in most regions (up to -3.2% in Hokkaido and Hokuriku). However, the projections reveal a net increase in the daily power demand in Okinawa and Kyushu, the two hottest regions (Figure 2a, Section 2). This increase is up to 1.6% in Kyushu and is even more pronounced in Okinawa (+1.6% for SSP1-2.6 and +11.1% for SSP5-8.5). Changes in the power demand across regions (except Okinawa) under SSP1-2.6 are small, ranging from -0.1 to 0.5%. Such results indicate that a decrease in the power demand in winter under future warming leads to an annual decrease in power demand in cold regions like Hokkaido. However, this possible decrease in winter power demand is overcompensated by a summer increase in hot regions such as Okinawa or Kyushu, leading to an annual increase.

Climate change's impact on carbon intensity also varies across regions (Figure 2d), but results are less significant than for power demand. Carbon intensity projections are less accurately simulated by our models (higher RMSE and lower R2). Nevertheless, the

projections show that most regions see their carbon intensity negatively affected by climate change. Tohoku and Shikoku, the regions with the highest average carbon intensity (roughly 600 gCO_2eq/kWh), are the only regions showing a climate-induced increase in carbon intensity under SSP3-7.0 and SSP5-8.5 (+1.3% and +2.3%, respectively). For Chugoku, Hokuriku, and Okinawa, the projected changes in carbon intensity are small and within the models' error range.

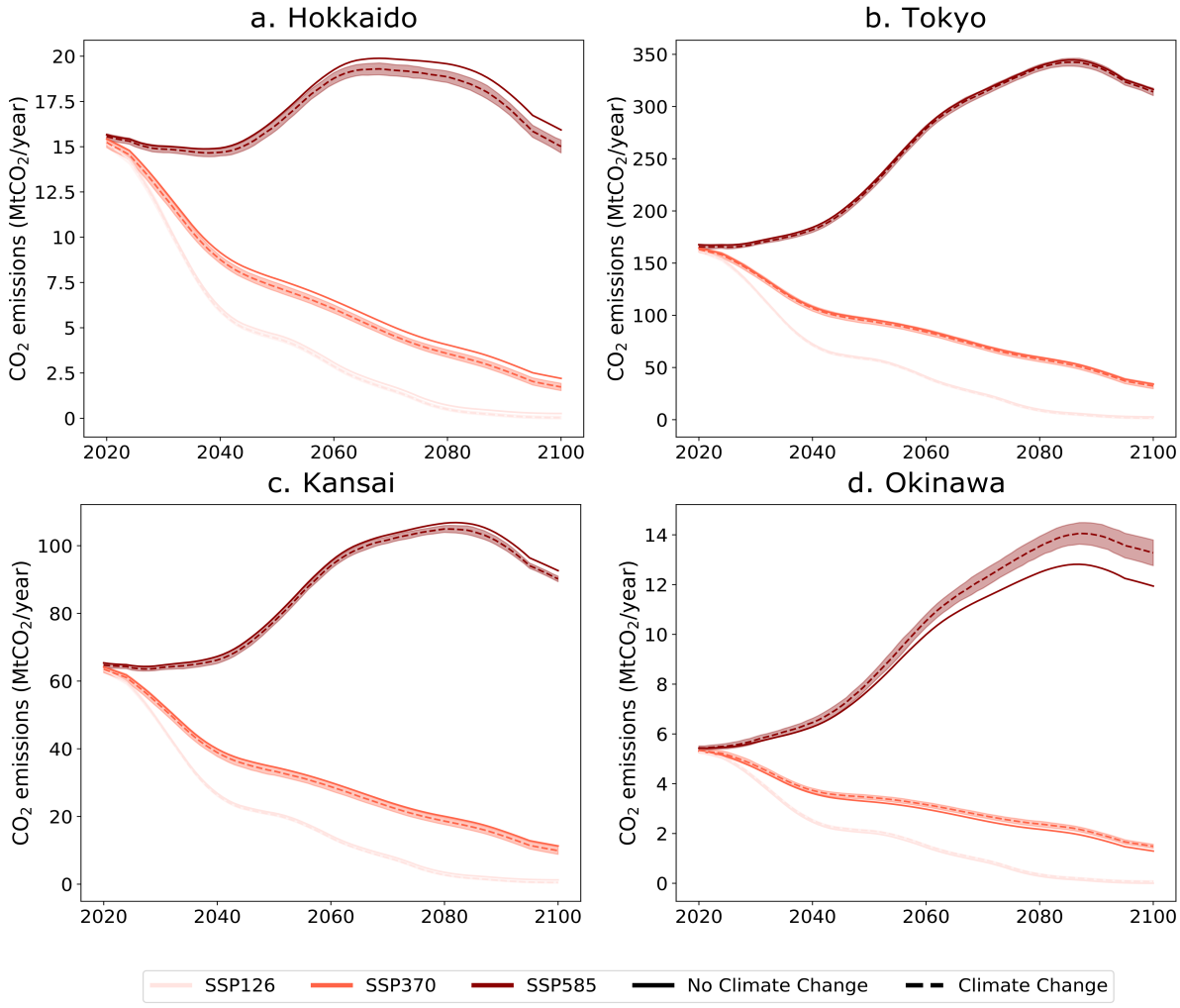

Figure 6. Annual CO_2 emissions from power generation under SSP1-2.6, SSP3-7.0, and SSP5-8.5, after considering socioeconomic impacts with (dashed line) and without (solid line) climate change impact for four regions: Hokkaido (a), Tokyo (b), Kansai (c) and Okinawa (d). The shaded area represents the 1-sigma standard deviation from the five climate models for the scenario considering climate change impact (dashed line).

Figure 6 shows how the influence of climate change on power demand and carbon intensity translates into carbon emissions. This figure shows the CO_2 projections considering socioeconomic factors (population, GDP, and environmental policies). The difference between the solid and dashed lines for each region and scenario represents the difference in emissions due to climate change alone. In Figure 6, we show the results of four regions. Results for the other regions are displayed in Figure S3 (Section S6, supplementary material). The regions with the most extreme temperatures (Hokkaido and Okinawa) indicate the largest differences. Climate change leads to a decrease in CO_2 emissions in Hokkaido but an increase in Okinawa. Okinawa and Shikoku are the only regions with higher emissions from climate change. The power demand is projected to increase strongly in Okinawa, especially under SSP5-8.5, which explains an increase in CO_2 emissions. On the other hand, the CO_2 emissions increase in Shikoku is due to an increase in carbon intensity simulated by the model. In all other regions, climate change leads to an increase in CO_2 emissions. In Kyushu, the CO_2 emissions decrease with climate change because the decline in carbon intensity takes over the increase in power demand. Such an effect can also be found in the Tokyo region, albeit to a lesser extent.

3.3 Attribution of the changes in power demand and CO_2 emissions

This section analyzes the effect of seasons and hot and cold periods on power demand and their respective contributions to the total annual change in power demand between 2020-2030 and 2090-2100. We divided days into four categories (cold, cool, warm, and hot) based on temperature distributions during 2016-2020. We calculated the number of days in each category under the three SSPs during 2020-2030 and 2090-2100. We attributed the contribution of the change in power demand in each category to the total change in power demand (Figure S4, section S7, supplementary material). The number of hot days increases in all ten regions. Increasing power demand during hot days is associated with cooling demand. However, such an increase is counterbalanced by a decrease in power demand in

other categories of days. Okinawa is an exception; power demand increases in all categories of days.

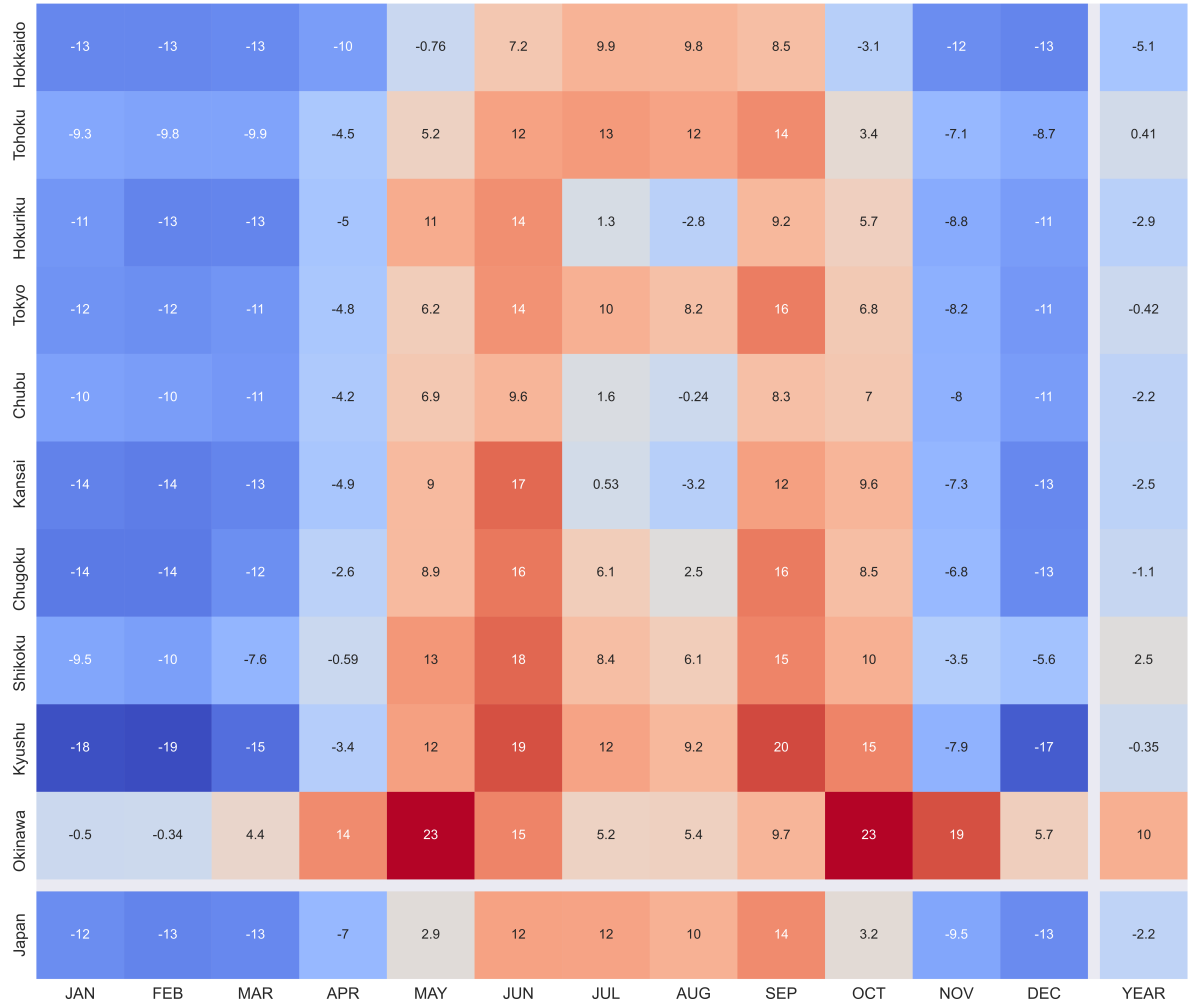

Figure 7. Monthly and regional changes (in percentage) in CO_2 emissions between the decade 2020-2030 and 2090-2100 due to climate impacts on future power demand. The mean results of the five models for SSP5-8.5 are shown.

Figure 7 shows the changes in CO_2 emissions between 2020-2030 and 2090-2100 due to changes in power demand and carbon intensity under SSP5-8.5 at monthly and regional levels. This figure allows for comparing our results with those of Hiruta et al. (2022b) (see Section 4 for the comparison). Most regions are projected to see a decrease in annual CO_2 emissions from power generation due to climate change, ranging from -0.3% to -5.1%. Shikoku and Okinawa are exceptions; their CO_2 emissions are projected to increase by 2.5

and 10%, respectively. Larger differences emerge at the monthly scale; the largest increases in CO_2 emissions (up to 23% increase in Okinawa) occur during a few transition months before and after the hottest months (i.e., May, June, September, and October) for all regions except Hokkaido and Tohoku. The largest increases occur during the warmest months in these two relatively cold regions. Such results indicate that the "next-warmest months" (May, June, September, and October) are most susceptible to future climate. A threshold temperature above which the demand for air conditioning starts was identified for each region in section 3.1 with partial dependence plots. Building on that, we formulate a possible explanation for the observed monthly changes; during July and August, the threshold temperatures triggering cooling demand are already exceeded for most days in all regions (except in Hokkaido and Tohoku). Thus, a further increase in power demand for cooling demand is not expected. However, with future warming, the temperature thresholds could be exceeded earlier in the year (in May or June) and longer (until September or October), explaining why the largest increase in power demand is projected to occur in the "next-warmest months". Similar monthly changes are observed for power demand but not for carbon intensity (Figures S5a and S5b, Section S8, supplementary material), indicating that monthly changes in regional CO_2 emissions are driven more by power demand than carbon intensity.

3.4 Comparison of different factors influencing CO_2 emissions of power generation

Figure 8 compares the impact of climate change on CO_2 emissions from power generation with those of socioeconomic factors (population, GDP, and carbon intensity). We quantified the amount of CO_2 emitted by each factor individually by varying one factor at a time. Note that the total in Figure 8 is the arithmetic sum of the individual changes from each factor, which is different from the total (with climate change) in Figure 6, calculated from the compounded change from all factors. With such a method, the results show that climate change plays a minor role in determining future changes in CO_2 emissions (Figure 8). The decreasing population under all scenarios negatively affects CO_2 emissions in all ten regions. GDP influences emissions in different directions according to scenarios; the GDP

effect is negative under SSP3-7.0 due to projected GDP decrease, whereas it is positive under SSP1-2.6 and SSP5-8.5 as GDP grows. Under SSP5-8.5, GDP is by far the most important factor determining CO_2 emissions in all ten regions. The effect of carbon intensity on CO_2 emissions is small under SSP5-8.5 and SSP3-7.0, as carbon intensity is not projected to decrease much in these scenarios. However, carbon intensity is the most important factor under SSP1-2.6, leading to a decrease in CO_2 emissions in most regions.

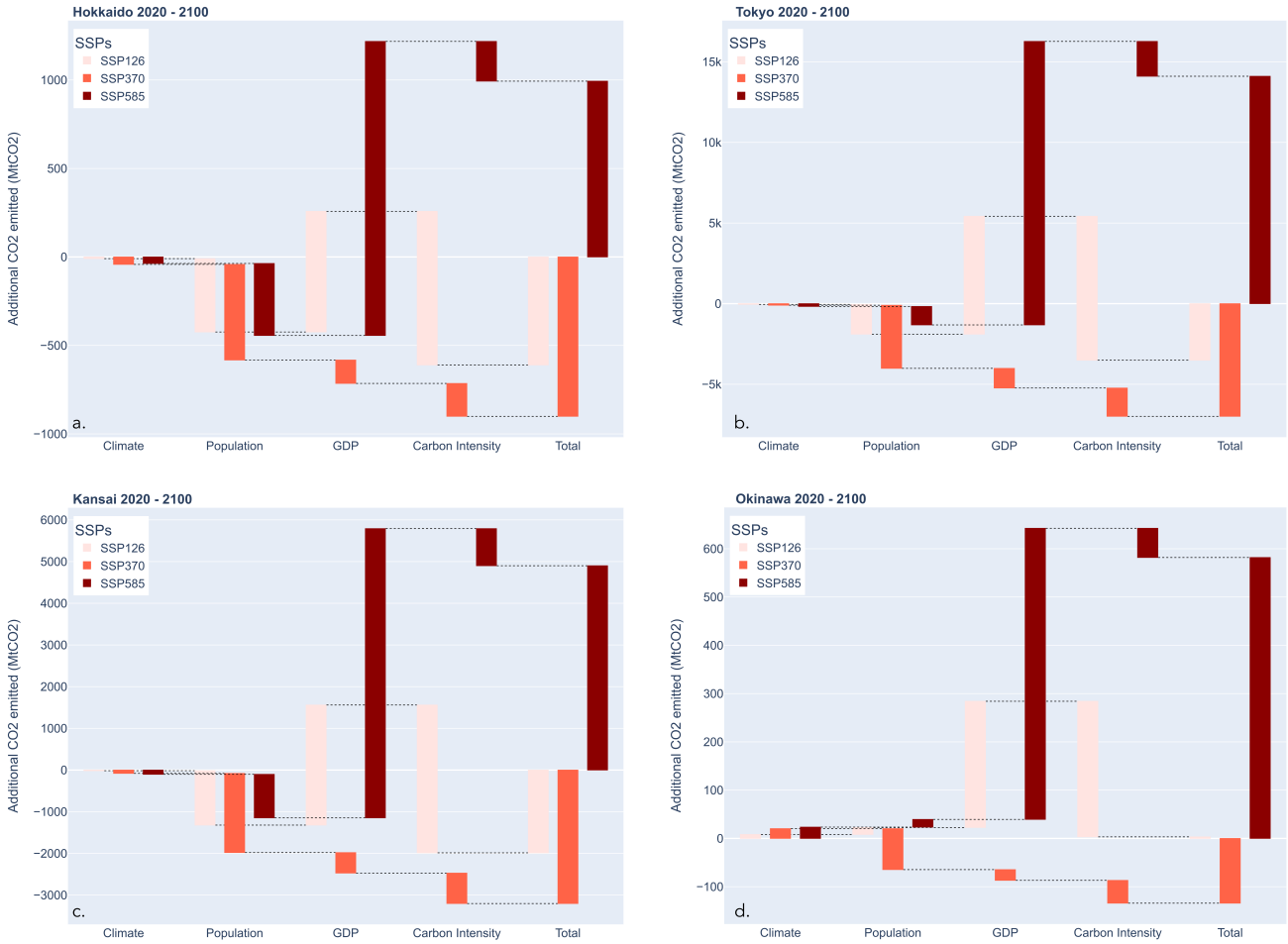

Figure 8. Individual contributions of changes in climate, population, GDP, and environmental policies to the changes in total CO_2 emissions of power generation over the period 2020-2100. The figure shows the change in CO_2 emissions due to each factor relative to the level with all other factors kept at current values. The figure shows the results for four representative regions from north to south: Hokkaido (a), Tokyo (b), Kansai (c), and Okinawa (d).

To summarize, when individual effects of climate, population, GDP, and carbon intensity on CO_2 emissions are considered separately, as in Figure 8, the climatic factor is overshadowed by the other factors. However, Figure 6 shows that climate change may have a significant impact when all factors are combined to project CO_2 emissions in certain regions under SSP5-8.5. The importance of the climate change impact on CO_2 emissions depends on the type of climate of the region and future climate scenarios; it also depends on the month of the year, as indicated in Figure 7.

4. Discussion

Our methodology allows for establishing regional statistical models that adequately reproduce the observations of daily power demand and carbon intensity. Seasonal cycles are well captured by the models for power demand, just as intra-weekly cycles (i.e., the distinction between working days and weekends). Interpretation methods such as partial dependence plots and Shapley values gave insights into understanding underlying mechanisms that control the dependency of power demand and carbon intensity on the predictors. As we are able to understand the impact of predictors on the outputs based on underlying mechanisms, such methods give us confidence in the projections of power demand and carbon intensity obtained using these models. Nevertheless, the models' inherent error is important for carbon intensity.

A well-known default of machine learning models is their bad performance outside their calibration range. For the projection, we calculated the percentage of days that have an average daily temperature outside the training temperature range period: 0.8% for SSP1-2.6, 3.6% for SSP3-7.0, and 5.2% for SSP5-8.5. For the projection period, we argue that the percentage of days with an average temperature outside the training range is small enough to avoid overfitting.

Hiruta et al. used a comparable methodology (Hiruta et al., 2022a) and also projected regional power demand in Japan with statistical models (Hiruta et al., 2022b). However, we

went one step further by modeling the influence of climate on carbon intensity and, eventually, CO_2 emissions. We obtained similar results for regional power demand; a decrease in power demand in cold regions and an increase in hot regions. However, we found a maximal increase in power demand during "next-warmest months" (May, June, September, and October). In contrast, the Hiruta study found it during the warmest months (July and August). This difference between the two studies has important implications for the power grid infrastructure in the future. Projecting the future power demand for air conditioning under changing climate is a critical issue in Japan, as revealed by the power supply situation in the summer of 2022. At the end of June 2022, Japan experienced a serious power deficit during weeks unusually hot for this month but not during equally hot weeks in July or August. The power deficit occurred in June as some thermal power plants were under periodic inspection before the high season and were not being operated (METI 2022). With climate change, there will be an increased risk of having peak demand earlier in the season. Power companies will have to consider it to avoid the problems of June 2022 happening again.

Here we discuss factors that can influence power demand but are not considered in our study. Firstly, the Urban Heat Island effect (UHI) is known to influence power demand. UHI amplifies power demand for air conditioning in densely populated cities in hot regions while it translates into a decrease in the demand for heating in colder regions (Xiaoma et al., 2019; Roxon, Ulm, and Pellenq, 2020). Xiaoma et al. (2019) showed that the UHI effect could increase the need for cooling energy by 19% and decrease the need for heating by 18.7% on average. According to the World Bank, 90% of the population lives in urban areas in Japan, with 60% of the country's 126 million inhabitants concentrated in the metropolitan areas of Tokyo, Nagoya, and Osaka. Hence, the UHI effect is probably not negligible and translates into a warming that is already a few degrees higher in cities than in rural areas (Takane et al., 2014; Takaya et al., 2014). The earth system models that generated the climate data we used for projection do not resolve UHI, implying that the future power demand in our projections may be underestimated in densely populated regions.

Secondly, a study by De Cian et al. (2019) predicts that almost 100% of Japanese homes will adopt air conditioning by mid-century for all scenarios. Even though Japan is already among the countries with the highest air conditioning adoption rate per household, about 90% nationwide in 2011 (De Cian et al., 2019), the effect of increased access to air conditioning was not taken into account in our model. Such an increase could boost power demand if all other factors, such as the efficiency of air conditioning and the housing insulation, are kept the same. Specifically, it could significantly change the climate response functions for power demand in cold regions like Hokkaido as, for now, these regions have fewer houses equipped with cooling systems compared to the rest of the country. However, our methodology lacks enough data to model the power demand linked to air conditioner usage in such regions.

Thirdly, human exposure indices use thresholds to account for the level of heat stress felt by the population. For the DI, there is no discomfort below 21; between 21 and 24, less than 50% of the population feels discomfort; between 24 and 27, more than 50% of the population feels discomfort; between 27 and 29, most of the population suffers discomfort; between 29 and 32, everyone feels severe stress; above 32, the state of medical emergency is reached (Stathopoulou et al., 2005). Figure 2b shows the projection for the annual maximal DI. The threshold of 24 has never been exceeded in Hokkaido for now. By the end of the century, DI could reach 27 in Hokkaido (Figure 2b). The maximal DI was 28 in Okinawa in 2020. At the end of the century, it could reach the dangerous threshold of 32. Exceeding such thresholds may lead to an underestimation of the power demand for air conditioning in all regions because there is no data to calibrate human behavior regarding the use of air conditioning when these thresholds are exceeded.

Finally, while our machine learning models developed to simulate the response of power demand to future climate are elaborated, how power demand responds to the future evolution of socioeconomic variables is modeled in a simpler way. Similarly, while we used

projections of climate variables with a rather high spatial resolution (CMIP6 data, widely used in the scientific community), the projections used for the socioeconomic variables were only at the national scale for GDP and carbon intensity. Given the data availability, there are differences in the spatial and temporal resolutions of climate and socioeconomic data used in our analysis, which might have affected the accuracy of power demand projections from our model.

References

Andrijevic, M. (2021). "Future cooling gap in shared socioeconomic pathways." *Environmental Research Letters* 16 (0940553). https://doi.org/10.1088/1748-9326/ac2195.

Auffhammer, M., Baylis, P., & Hausman, C.H. (2016). "Climate change is projected to have severe impacts on the frequency and intensity of peak electricity demand across the United States" *PNAS* 114 (8) 1886-1891

A-PLAT. (2022). https://adaptation-platform.nies.go.jp/en/ 2824

Breiman, L. (2001). "Random Forests." *Machine Learning* 45:5-32. 10.1023/A:1010933404324.

Buzan, J.R., Oleson, K., & Huber, M. (2014). "Implementation and comparison of a suite of heat stress metrics within the Community Land Model version 4.5" *Geosci. Model Dev. Discussions* 7, 5197–5248, 10.5194/gmdd-7-5197-2014

CDS 2020. https://cds.climate.copernicus.eu/#!/home

De Cian, E., Pavanello, F., Randazzo, T., Mistry, M., & Davide, M. (2019). "Households' adaptation in a warming climate. Air conditioning and thermal insulation choices." *Environmental Science and Policy* 100:136-157. https://doi.org/10.1016/j.envsci.2019.06.015.

Dellink, R., Chateau, J., Lanzi, E., & Magné, B. (2017). "Long-term economic growth projections in the Shared Socioeconomic Pathways." *Glob. Environ. Change* 42, 200–214.

Epstein, Y. & Moran, D.S. (2006). "Thermal comfort and heat stress indices" *Industrial Health* 44 388-398 https://doi.org/10.2486/indhealth.44.388

Friedman, J.H. (1991). "Multivariate Adaptive Regression Splines." *Annals of Statistics* 19 (March): pp. 1–67. 10.1214/aos/1176347963.

Friedman, J.H. (1999). "Stochastic gradient boosting." *Computational Statistics and Data Analysis* 38:367-378. 10.1016/S0167-9473(01)00065-2.

Hiruta, Y., Gao, L. , & Ashina, S. (2022a). "A novel method for acquiring rigorous temperature response functions for electricity demand at a regional scale." *Science of the Total Environment* 819:152893. https://doi.org/10.1016/j.scitotenv.2021.152893.

Hiruta, Y., Ishizaki, N. N., Ashina, S., & Takahashi, K. (2022b). "Regional and temporal variations in the impacts of future climate change on Japanese electricity demand: Simultaneous interactions among multiple factors considered." *Energy Conversion and Management: X* 14:100172. https://doi.org/10.1016/j.ecmx.2021.100172.

Ho, T. K. (1995). "Random Decision Forests." *Proceedings of the 3rd International Conference on Document Analysis and Recognition*, (August), pp. 278–282. 10.1109/ICDAR.1995.598994.

IEA. (2022). "Data and Statistics - Electricity information" https://www.iea.org/data-and-statistics/data-product/electricity-information#data-sets

IMF. (2022). "World Economy Outlook (October 2022)" https://www.imf.org/external/datamapper/datasets/WEO

Lange, S. (2021). "ISIMIP3b bias adjustment fact sheet Contents." ISIMIP.https://www.isimip.org/documents/413/ISIMIP3b_bias_adjustment_fact_sheet_Gnsz7CO.pdf.

Maia-Silva, D., Kumar, R. & Nateghi, R. (2020). "The critical role of humidity in modeling summer electricity demand across the United state." *Nature Communications* 11:1686 https://doi.org/10.1038/s41467-020-15393-8

METI. (2022). "Electricity Supply and Demand Measures for FY2022" Agency for Natural Resources and Energy of the Ministry of Economy Trade and Industry. https://www.meti.go.jp/shingikai/enecho/denryoku_gas/denryoku_gas/pdf/052_04_03.pdf

Mora, C., et al. (2017). "Global risk of deadly heat." *Nature Climate Change* 7:501-506. 10.1038/NCLIMATE3322.

Molnar C. (2020). "Interpretable Machine Learning" lulu.com

Muñoz Sabater, J. (2019). "ERA5-Land hourly data from 1981 to present. Copernicus Climate Change Service (C3S) Climate Data Store (CDS)." 10.24381/cds.e2161bac.

Patel, L. (2022). "Climate Change and Extreme Heat Events: How Health Systems Should Prepare." *NEJM Catalyst Innovations in Care Delivery* 3 (7). https://doi.org/10.1056/CAT.21.0454.

Riahi, K., van Vuuren, D.P., Kriegler, E., Edmonds, J., O'Neill, B.C., Fujimori, S., Bauer, N., Calvin, K., Dellink, R., Fricko, O., et al. (2017). "The Shared Socioeconomic Pathways and their energy, land use, and greenhouse gas emissions implications: An overview." *Glob. Environ. Change* 42, 153–168.

Roxon, J., Ulm, F-J ., & Pellenq, R.J.M. (2020). "Urban heat island impact on state residential energy cost and CO2 emissions in the United States." *Urban Climate* 31:100546. https://doi.org/10.1016/j.uclim.2019.100546.

Sohar, E., Adar, R., Kaly, L. (1963). "Comparison of the environmental heat load in various part of Israel" *Bull Res Counc. Israel* 10, 111-115

Stathopoulou, M., Cartalis, C., Keramitsoglou, I., & Santamouris, M. (2005). "Thermal remote sensing of Thom's Discomfort Index (DI): Comparison with in situ measurements." *Proc SPIE* 5983:131-139. 10.1117/12.627541.

Takane Y., Kusaka, H. & Kondo, H. (2014). Investigation of a recent extreme high-temperature event in the Tokyo metropolitan area using numerical simulations: the potential role of a 'hybrid' foehn wind, Q. J. R. Meteorol. Soc., DOI: 10.1002/qj.2490.

Takaya A., Morioka Y. & Behera, S. K. (2014). Role of climate variability in the heatstroke death rates of Kanto region in Japan, Scientific Reports, DOI: 10.1038/srep05655.

Thom, E.C. (1959). "The Discomfort Index." *Weatherwise* 12:57-61. https://doi.org/10.1080/00431672.1959.9926960.

Van Ruijven, B., De Cian, E. & Wing, I.S. (2019). "Amplification of future energy demand growth due to climate change." *Nature Communications* 10:2762. https://doi.org/10.1038/s41467-019-10399-3.

Van Vuuren, D., Stehfest, E., Gernaat, D., et al. (2021). “The 2021 SSP scenarios of the IMAGE3.2 model.” *The Hague: PBL Netherlands Environmental Assessment Agency* 4740. 10.31223/X5CG92.

Xiaoma, L., Yuyu, Z., Sha, Y., Gensuo, J., Huidong, L. & Wenliang, L. (2019). "Urban heat island impacts on building energy consumption: a review of approaches and findings." *Energy* 174:407-419. https://doi.org/10.1016/j.energy.2019.02.183.

Yalew, S., et al. (2020). "Impacts of climate change on energy systems in global and regional scenarios." *Nature Energy* 5:794-802. https://doi.org/10.1038/s41560-020-0664-z.

Zittis, G. (2021). "Business-as-usual will lead to super and ultra-extreme heatwaves in the Middle East and North Africa." *Climate and Atmospheric Science* 4:20. https://doi.org/10.1038/s41612-021-00178-7.

Licensee